Environ. Sci. Technol. **2005**, *39,* 8803−8811

Dissolution of Composition B Detonation Residuals

J. H. LEVER,*,† S. TAYLOR,† L. PEROVICH,† K. BJELLA,† AND B. PACKER‡

U. S. Army Engineer Research and Development Center, 72 Lyme Road, Hanover, New Hampshire 03755, and U. S. Army Environmental Center, Aberdeen Proving Ground Maryland 21010

Composition B (Comp B) detonation residuals pose environmental concern to the U. S. Army because hexahydro-1,3,5-trinitro-1,3,5-triazine (RDX), a constituent, has contaminated groundwater near training ranges. To mimic their dissolution on surface soils, we dripped water at 0.51 mL/h onto individual Comp B particles (0.1−2.0 mg) collected from the detonation of 81-mm mortars. Analyses of the effluent indicate that the RDX and 2,4,6-trinitrotoluene (TNT) in Comp B do not dissolve independently. Rather, the relatively slow dissolution of RDX controls dissolution of the particle as a whole by limiting the exposed area of TNT. Two dissolution models, a published steady-flow model and a drop-impingement model developed here, provide good agreement with the data using RDX parameters for time scaling. They predict dissolution times of 6−600 rainfall days for 0.01−100 mg Comp B particles exposed to 0.55 cm/h rainfall rate. These models should bracket the flow regimes for dissolution of detonation residuals on soils, but they require additional data to validate them across the range of particle sizes and rainfall rates of interest.

Introduction

Composition B (Comp B) is a 60/39 mixture of hexahydro-1,3,5-trinitro-1,3,5-triazine (RDX) and 2,4,6-trinitrotoluene (TNT) that contains ∼1% wax. It has been used in munitions since World War II for its high explosive yield. However, it poses environmental concern to the U. S. Army because RDX is known to have contaminated groundwater beneath impact areas at Massachusetts Military Reservation, MA. (*1*) and Fort Lewis, WA (*2*).

Taylor et al. (*3*, *4*) showed that detonations scatter high-explosive (HE) residuals on ranges as sub-millimeter- to centimeter-sized particles, with mean size dependent on the proportional yield of the detonation. Areal concentrations decreased with distance but were less than one particle per square centimeter. These observations are consistent with soil and snow samples that show large, spatially heterogeneous variations in HE concentrations on ranges (*5*, *6*).

Dissolution of RDX, rather than its subsequent aqueous transport, probably controls the rate of the chemical's entry into the groundwater. This is because the absorption coefficient for RDX in soil is low (*7*), indicating that RDX will move with the water at the infiltration rate. For sandy soils and shallow aquifers, rainfall reaches the groundwater in days to weeks while the dissolution of millimeter-sized particles will take months to years. Once it is dissolved, factors that influence RDX groundwater concentrations include dispersion and dilution.

The dissolution rate of Comp B detonation residuals depends on variables that include the solubility of its constituents, the rainfall rate, and the surface area and composition of the particle (both of which can change as the particle dissolves). Of these variables, the solubility of RDX and of TNT are well constrained (*8*, *9*), while the mass, size, and surface area distributions of HE residuals have been measured for just a few detonations (*3*, *4*).

Several attempts have been made to measure the dissolution rate of Comp B and its constituents. Lynch et al. (*10*, *11*) stirred fixed water volumes to measure the initial dissolution rates of RDX and TNT particles independently, in unbound mixtures and as molded Comp B particles. Phelan et al. (*12*) measured dissolution rates for layers of Comp B particles within columns of glass beads subjected to steady porous flow.

We have taken a new approach. We collected Comp B residuals from low-order field detonations and characterized 30 particles to determine their structure and compositional variability. We then dripped water on four individual Comp B particles and tracked changes in their surface textures, compositions, and dissolution rates with time. These tests mimic common field conditions on training ranges, where rainfall dissolves spatially isolated HE particles on the soil surface. Last, we simulated the dissolution experiments using two models that correspond to slow and fast percolation of rainfall into soil.

Materials and Methods

Comp B Samples. We collected Comp B particles from two blow-in-place, low-order detonations of 81-mm mortars, designated LO-a and LO-b (*13*, *4*). To avoid entraining soil, the munitions were detonated on top of a thick steel table centered on a 15 × 15-m^2 flame-resistant vinyl tarp (*13*). We collected the residuals on aluminum trays (66 × 46 cm^2) located on the tarp.

Taylor et al. (*4*) noted that Comp B particles from low-order detonations individually had different RDX/TNT ratios. For this work, we measured the variability in 30 randomly selected particles. Each particle was weighed on a Mettler Toledo MX5 microbalance, photographed, and then dissolved in 1 mL of acetonitrile. The dissolved sample was added to 3 mL of distilled water, and the samples were filtered through a 0.45-μm Millipore cartridge. We used high performance liquid chromatography (HPLC), which separates HMX, RDX, TNT, DNT, and their co-contaminants, to analyze the samples. We followed method 8330 (*14*), the standard method for determining explosive residuals in water. A Water NovaPak C8 column was eluted at 1.4 mL/min (28 °C) with 85:15 water/2-propanol mix and detected by UV at 254 nm. Commercially available standards (Restek) specifically developed for method 8330 were used for calibration. This work provided a measure of the RDX/TNT variability in the 30 Comp B particles, a correlation between the measured and the estimated (from photographs) particle mass, and a check on our analytical methods.

Dissolution Tests. We selected four Comp B particles for dissolution experiments. The long duration of each test and the availability of only one apparatus limited the number of tests. Particles 2 and 4 were weighted on a Mettler Toledo

* Corresponding author phone (603)646-4309; fax: (603)646-4477; e-mail: james.h.lever@erdc.uscae.army.mil.
† U. S. Army Engineer Research and Development Center.
‡ U. S. Army Environmental Center.

10.1021/es050511r Published on Web 10/13/2005

Report Documentation Page

Form Approved
OMB No. 0704-0188

1. REPORT DATE	2. REPORT TYPE	3. DATES COVERED
2005		**00-00-2005 to 00-00-2005**

4. TITLE AND SUBTITLE	5a. CONTRACT NUMBER
Dissolution Of Composition B Detonation Residuals	5b. GRANT NUMBER
	5c. PROGRAM ELEMENT NUMBER
6. AUTHOR(S)	5d. PROJECT NUMBER
	5e. TASK NUMBER
	5f. WORK UNIT NUMBER
7. PERFORMING ORGANIZATION NAME(S) AND ADDRESS(ES) **U. S. Army Engineer Research and Development Center,72 Lyme Road,Hanover,NH,03755**	8. PERFORMING ORGANIZATION REPORT NUMBER
9. SPONSORING/MONITORING AGENCY NAME(S) AND ADDRESS(ES)	10. SPONSOR/MONITOR'S ACRONYM(S)
	11. SPONSOR/MONITOR'S REPORT NUMBER(S)

12. DISTRIBUTION/AVAILABILITY STATEMENT
Approved for public release; distribution unlimited

13. SUPPLEMENTARY NOTES
Environ. Sci. Technol. 2005, vol 39,NO. 22, pages 8803-8811

14. ABSTRACT

Composition B (Comp B) detonation residuals pose environmental concern to the U. S. Army because hexahydro-1,3,5-trinitro-1,3,5-triazine (RDX), a constituent, has contaminated groundwater near training ranges. To mimic their dissolution on surface soils, we dripped water at 0.51 mL/h onto individual Comp B particles (0.1-2.0 mg) collected from the detonation of 81-mm mortars. Analyses of the effluent indicate that the RDX and 2,4,6-trinitrotoluene (TNT) in Comp B do not dissolve independently. Rather, the relatively slow dissolution of RDX controls dissolution of the particle as a whole by limiting the exposed area of TNT. Two dissolution models, a published steady-flow model and a drop-impingement model developed here, provide good agreement with the data using RDX parameters for time scaling. They predict dissolution times of 6-600 rainfall days for 0.01-100 mg Comp B particles exposed to 0.55 cm/h rainfall rate. These models should bracket the flow regimes for dissolution of detonation residuals on soils but they require additional data to validate them across the range of particle sizes and rainfall rates of interest.

15. SUBJECT TERMS

16. SECURITY CLASSIFICATION OF:			17. LIMITATION OF ABSTRACT	18. NUMBER OF PAGES	19a. NAME OF RESPONSIBLE PERSON
a. REPORT **unclassified**	b. ABSTRACT **unclassified**	c. THIS PAGE **unclassified**	**Same as Report (SAR)**	**9**	

MX5 microbalance before and after the tests. Unfortunately, we did not measure the initial mass of Particle 1, although we did measure its total dissolved mass and mass after the test, which sum to the total HE mass. Also, we measured the initial mass of Particle 3 but later lost it while removing it from the apparatus for photographing.

For each test, we placed a single Comp B particle on a porous glass frit at the base of a glass holder (11 mm in diameter × 25 mm high) with a luer lock at its top. To the luer lock, we connected a 20-mL syringe mounted in a syringe pump. The syringe dripped 0.51 mL/h of Milli-Q distilled water (pH 6) onto the Comp B particle (equivalent rainfall rate of 0.55 cm/h). The timed arrival rate of the drops was fairly steady at 20 ± 1 drops/h. The water flowed through the frit into precleaned test tubes mounted in a fraction collector. The room temperature was 22 ± 1 °C. The fraction collector moved an empty tube into position under the frit every 2 h, yielding a series of 1-mL samples, which when analyzed, gave us the RDX and TNT concentrations in the effluent as a functions of time. At intervals, we transferred the particle from the frit to a glass dish using a fine-haired paint brush and air-dried and photographed it to observe surface changes before continuing the dissolution test. The procedure took about 15 min. We replaced the glass frit and cleaned the glass holder between tests.

The water samples were collected daily and prepared for HPLC analysis. We added 2 mL of distilled water and 1 mL of acetonitrile to each 1-mL sample. The standards were prepared using the same ratio of acetonitrile to water. The samples were filtered into 2-mL vials and stored in a refrigerator until analyzed (usually within a week). We used the same configuration of the HPLC for analysis as described above.

Results

Comp B Samples. We applied tetra-butylammonium hydroxide, a reagent that reacts with TNT to form a red product, on sections of Comp B grains to observe the size and texture differences between RDX and TNT crystals. Both optical and electron-microscope images show that Comp B contains ~100-μm RDX crystals in a matrix of fine-grained TNT and is not a homogeneous mixture (*4*). Consequently, individual particles can vary in their proportions of RDX and TNT. Table 1 shows this variability for 30 Comp B particles from detonation LO-a.

The average RDX to TNT ratio for the 30 particles was 1.74 ± 0.28, higher than the bulk Comp B average of 60/39 = 1.54. We recovered, on average, 96 ± 1% of the weighed mass when we dissolved and analyzed the particle for HE components. The mass not recovered may include wax from the manufacturing or dirt and metal often seen on the particle's surface (Figure 1).

We estimated each particle's mass using its measured major and minor axes and assuming its shape to approximate a prolate spheroid of density 1.65 g/cm^3 (*15*). The average ratio of estimated mass to measured mass was an encouraging 1.03 ± 0.47. This result is helpful when converting size distributions measured for detonation residuals to corresponding mass distributions (*3*, *4*).

Dissolution Tests. Table 2 summarizes the results for the four particle-dissolution tests. Photographs before dissolution revealed a different appearance for each particle, which we attribute to different heating histories through the detonations. The average flow rate of 0.51 ± 0.01 mL/h produced ~20 drops per hour with an average size of 4 mm. This was larger than the 1.4-mm mass-average raindrop size expected for the equivalent 0.55 cm/h rainfall rate (*16*). The Comp B particles were free to move around on the filter and were, therefore, not struck directly by every drop.

TABLE 1. Analysis of 30 Comp B Particles Recovered from Detonation LO-a (81-mm Mortar)

measured mass (μg)	RDX/ TNT ratio	mass fraction recovered by HPLC	mass estimated from particle dimensions (μg)	mass ratio estimated/ measured
1855	1.48	0.96	2260	1.22
2931	1.53	0.95	4510	1.54
1486	1.60	0.95	1340	0.90
2379	1.57	0.95	2070	0.87
1495	1.69	0.96	2200	1.47
1975	1.62	0.96	2160	1.09
10160	1.95	0.99	16600	1.64
941	1.94	0.94	633	0.67
595	1.99	0.95	402	0.68
366	2.48	0.98	359	0.98
420	1.52	0.94	302	0.72
251	2.17	0.96	213	0.85
369	2.22	0.97	307	0.83
857	2.23	0.95	1870	2.18
972	1.62	0.95	712	0.73
1225	1.64	0.96	1230	1.00
1133	1.64	0.96	752	0.66
976	1.66	0.95	640	0.66
13556	1.99	0.98	19200	1.42
1899	1.55	0.96	1170	0.62
28034	1.40	0.95	37100	1.32
779	1.79	0.97	648	0.83
533	1.83	0.97	541	1.02
924	1.41	0.94	680	0.74
237	1.62	0.96	148	0.62
2704	1.72	0.95	6620	2.45
936	1.59	0.96	470	0.50
697	1.48	0.94	434	0.62
814	1.42	0.96	621	0.76
6672	1.94	0.95	9280	1.39
average	1.74	0.96		1.03
std dev	0.28	0.01		0.47

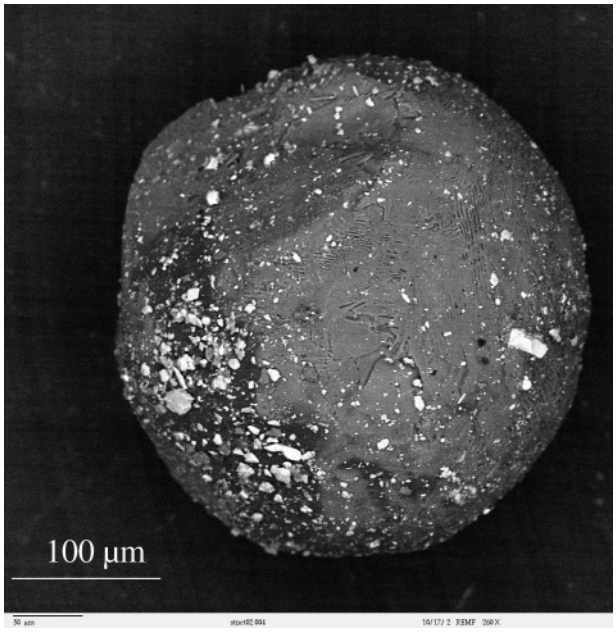

FIGURE 1. Micrograph showing metal, soil, and soot (very dark areas) adhering to a Comp B particle from a low-order detonation.

Test 1. Particle 1 initially measured 2.1 × 1.4 × 0.96 mm^3 and was from detonation LO-a. Although we did not weigh it initially, the analyzed dissolved mass plus the end mass indicate an initial HE mass of 1821 μg. Concentrations of TNT in the effluent were high during the first 24 h, 6 mg/L for TNT compared with 3 mg/L for RDX. These values were

TABLE 2. Summary of Conditions for Dissolution Tests

	Test 1	Test 2	Test 3	Test 4
particle from detonation	LO-a	LO-b	LO-b	LO-b
particle dimensions (μm)	2150 × 1400 × 960	430 × 420 × 330	700 × 550 × 400	1350 × 925 × 900
initial mass (μg)	1821[a]	102	276	1153
test duration (days)	68	16	11	42
total water volume (mL)	847	191.5	127.5	403
water flow rate (mL/h)	0.518	0.505	0.501	0.512
mass dissolved (μg)	1730	52.6	76	383
dissolved RDX/TNT	1.72	0.80	0.96	0.84
end mass (μg)	92	35	particle lost	701
end RDX proportion (%)	99	69	?	66
total recovered RDX/TNT	1.86	1.19	?	1.43
mass recovered (%)	92	85.9	?	94.0
mass dissolved/initial mass	0.87	0.52	0.28	0.33

[a] Sum of the HE mass dissolved and the end mass.

TABLE 3. Model Parameters for RDX and TNT in Water at 25 °C

parameter	RDX	TNT	Comp B	source
S_j (g/cm^3)	4.6×10^{-5}	1.3×10^{-4}		(*9, 21*)
D_j (cm^2/s)	2.2×10^{-6}	6.7×10^{-6}		(*10, 21*)
ρ_j (g/cm^3)	measured	measured	1.65	(*15, 21*)

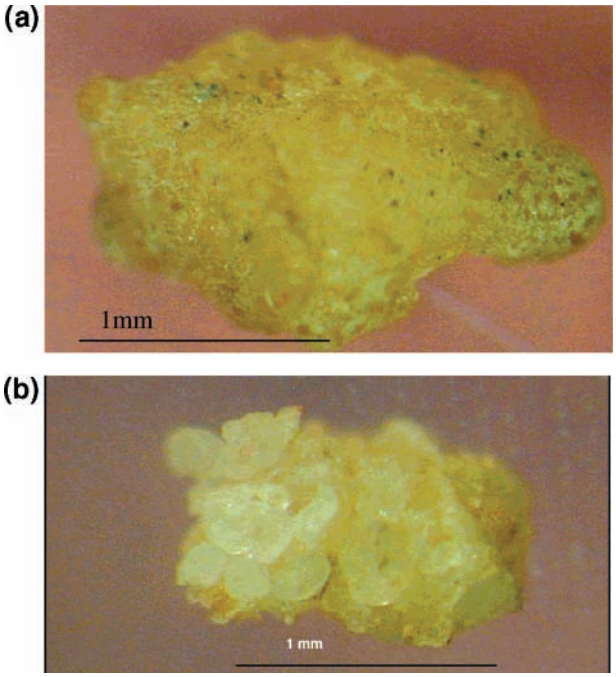

FIGURE 2. Micrographs of Particle 1 (a) before dissolution and (b) after dissolution for 68 days, at which point the particle was 99% RDX.

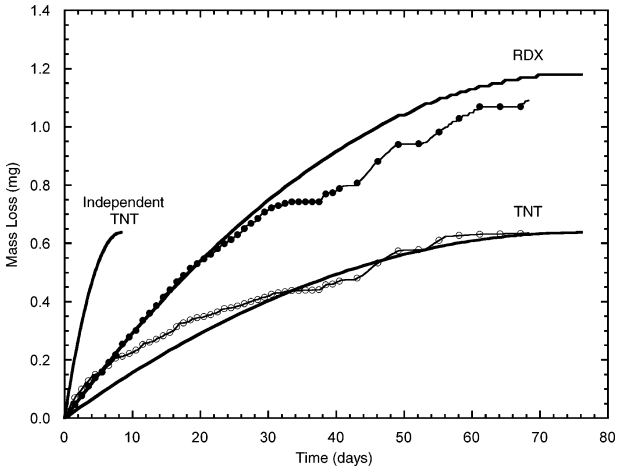

FIGURE 3. Dissolution of Particle 1 measured (symbols) and modeled for slow percolation (smooth lines). The predicted independent dissolution of TNT is too fast and does not track that of RDX. At the end of the test, the 0.092-mg particle was 99% RDX, accounting for the gap between the predicted and the measured results.

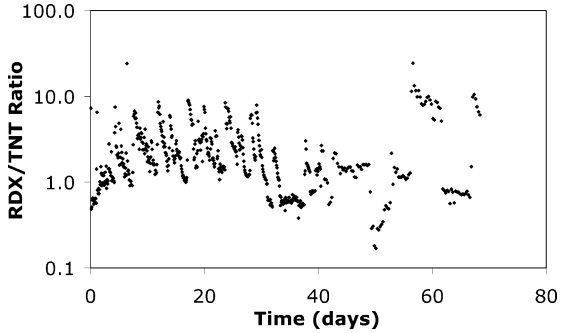

FIGURE 4. RDX/TNT ratio for 580 individual effluent samples collected from Particle 1.

well below their respective solubility limits in water (Table 3). During this period, the particle's surface texture changed from smooth to bumpy (Figure 2). The change in surface texture and the elevated TNT concentrations at the beginning of the experiment were due to preferential dissolution of the surface TNT that exposed some of the RDX crystals. The TNT mass-loss rate then steadily decreased until it was about half of the RDX value (Figure 3).

The ratio of RDX/TNT dissolved in each of the 580 water samples varied over a factor of 8 around a long-term average of 1.72 (Figure 4), apparently reflecting the relative exposed surfaces of the RDX and TNT constituents. Some RDX crystals (typically about 0.1 mm in size) also broke free from the main particle. Clearly, particle dissolution did not proceed as if the RDX and TNT were homogeneously mixed and dissolving independently. Bulk Comp B can contain ~ 5% HMX, a byproduct of the RDX manufacturing. Less than 1% HMX was recovered from this particle, suggesting that HMX-free RDX was used for this round. We also saw very little 2Am-DNT and 4Am-DNT, the breakdown products of TNT, because the water samples were analyzed promptly.

Test 2. Particle 2 initially weighed 102 μg and was from detonation LO-b. Its round shape and smooth exterior indicated that at least the outer surface of the particle had melted. We saw low concentrations of TNT and hardly any RDX for the first 2 days of the experiment (Figure 5). Photographs of the particle also show relatively little change

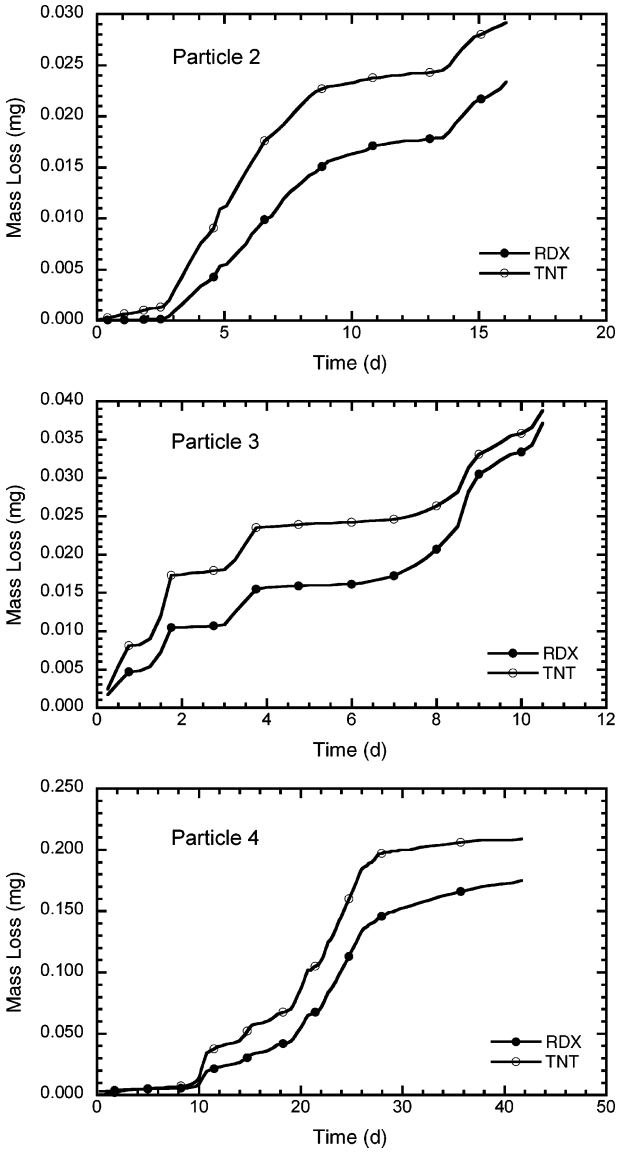

FIGURE 5. Mass loss vs time for Particles 2, 3, and 4.

in the surface appearance. Wax initially used to coat the RDX crystals during manufacture may have concentrated at the surface as the particle was formed by the detonation. Starting at day 2.8, however, both the TNT and the RDX concentrations increased by 1−2 orders of magnitude. Photographs revealed that part of the smooth surface was gone and that RDX crystals were exposed. After 5 days, a portion of the outer smooth surface was still present on one side of the particle. The RDX/TNT in the dissolved mass averaged 0.80, which increased to 1.19 with the addition of the end mass. The RDX/TNT ratio of individual effluent samples also varied by an order of magnitude but showed fewer cycles than Particle 1.

Test 3. Particle 3 initially weighed 276 μg and was from LO-b. The experiment was short-lived because we lost the particle while attempting to photograph it. This particle had a dark smooth exterior, which looked melted. Unlike Particle 2, however, it immediately began to dissolve. Like the other tests, the HE concentrations in the water samples showed a step dissolution pattern, and the RDX and TNT mass losses tracked each other (Figure 5). The RDX/TNT ratio calculated from the dissolved mass was 0.96, with individual samples again showing an order of magnitude variation.

Test 4. Particle 4 initially weighed 1153 μg and was also from LO-b. This lumpy particle had been heated, but may not have been melted, by the detonation. Similar to Test 2, there was a period at the beginning of the experiment when both RDX and TNT dissolved very slowly (Figure 5). Photographs showed that the particle became lighter colored on day 9, indicating loss of its dark, soot-containing surface. Individual RDX crystals were evident on day 12. These changes in the particle's appearance coincided with large increases in the dissolution rates. The RDX and TNT concentrations again tended to track each other. The RDX/TNT in the dissolved mass averaged 0.84, which increased to 1.43 with the addition of the end mass. The RDX/TNT ratio in individual samples showed a fairly steady increase during this test, although the test may have been too short to observe large fluctuations in this ratio characteristic of the other tests.

Dissolution Models. The drip experiment mimics a raindrop falling on or near an HE particle lying on porous soil. When a water droplet strikes the surface, it wets the particle and inundates the surface to some depth. The water then percolates into the soil or runs off overland. Stable-isotope measurements (summarized in refs *17* and *18*) indicate that most rainfall percolates directly into the soil and little runs overland into rivers, except in areas having highly impermeable surfaces (e.g., urban areas, exposed rock). This is true even during heavy rainstorms. Consequently, on the time scale of a storm (hours) rainfall rates approximate infiltration rates. However, water can pool on the soil surface between the arrival of raindrops at a given location (seconds to minutes). The depth of water will depend on the percolation rate relative to the rainfall rate, and this relative rate establishes the two regimes that we model here for dissolution of Comp B.

Slow Percolation: Steady-Flow Dissolution Model. When the percolation rate of water into the soil is slow, water will pool on the surface during a rainstorm. The mean flow velocity of water past an exposed HE particle will then approximate the average rainfall rate during the storm.

Chambre et al. (*19*, *20*) developed an analytical model for the dissolution of low-solubility species from a cylindrical waste form imbedded in porous rock or soil. Matyskiela (*21*) applied this model to predict dissolution rates of Comp B particles in soil under the assumption that the RDX and TNT components dissolve independently. The model assumes that under steady conditions the dissolved concentration of a species at the solid−water interface is the solubility limit for that species. It was developed for the case of a long cylinder of radius R perpendicular to the mean flow and assumes that the flow field derives from Darcy's potential flow in the porous medium, with U the pore velocity far from the cylinder. It solves the case of large Peclet number, $Pe = UR/D_j > 4$, where D_j is the diffusion coefficient of species j, then applies the calculated average mass flux over the surface of a finite cylinder. The resulting steady-state dissolution rate, m_j (g/s), of species j is

$$m_j = 8\pi^{-1/2}\phi S_j (D_j U)^{1/2}(1 + R/L)/(R/L)(\mathrm{AF})R^{3/2} \quad (1)$$

where ϕ is the soil porosity, S_j is the solubility limit of species j in water (g/cm^3), D_j is the diffusion coefficient of species j in water (cm^2/s), U is the far-field pore velocity (cm/s), R is the cylinder radius (cm), L is the cylinder length (cm), and AF is the area factor, introduced here to allow particle surface area to differ from that of a smooth cylinder (AF = 1)

We may apply this model here for the case of $\phi = 1$ because the mean percolation rate is low (Reynolds number $\ll 1$). Also, Chambre et al. (*19*) indicate that dissolution reaches steady state for time $t > 1.2R/U$. For $U = 0.55$ cm/h, all particles would reach steady-state dissolution in less than 0.1 h, very short compared with the run time of the experiments.

The mass of species j in the particle at any time is

$$M_j = \rho_j \frac{4}{3}\pi R^3/(R/L) \quad (2)$$

where ρ_j is the density of j in Comp B. To determine the change in particle size with time, we may differentiate eq 2 and set it equal to the negative of eq 1. A simplifying assumption is that cylinder aspect ratio, R/L, remains constant. The change in particle size with time t thus becomes

$$R^{3/2} = R_0^{3/2} - B_j t \quad (3)$$

where R_0 is the initial radius and

$$B_j = 4\pi^{-3/2}\phi(S_j/\rho_j)(D_j U)^{1/2}(1 + R/L)\mathrm{AF}$$

Comparing eqs 1 and 3, we find that the predicted dissolution rate decreases linearly with time.

The heterogeneous nature of Comp B particles caused the instantaneous dissolution rates and the RDX/TNT ratios to vary significantly about mean values. Because we are concerned with overall trends, we compare the measured and predicted cumulative dissolution or mass loss, $M_{\mathrm{loss}j}$, versus time, which integrates these variations

$$M_{\mathrm{loss}j} = A_j(R_0^{3/2}t - B_j t^2/2) \quad (4)$$

where $A_j = 8\pi^{-1/2}\phi S_j(D_j U)^{1/2}(1 + R/L)/(R/L)\mathrm{AF} = m_j/R^{3/2}$ To apply this model, we calculated the equivalent cylinder for each particle, preserving the measured initial mass and minor-axis/length ratio. We also used the measured RDX/TNT ratio for each particle (Table 2) because they varied from the nominal Comp B average of 1.54. Table 3 summarizes other parameters used.

As written, eq 4 allows independent dissolution of RDX and TNT by selection of species-specific parameters S_j, D_j, and ρ_j. However, the drip experiments indicate dissolution of RDX controls the dissolution of Comp B, and the particle approximately preserves its mean RDX/TNT ratio throughout dissolution. To implement this approximation, we use RDX parameters in eq 4 and preserve the mean RDX/TNT ratio

$$M_{\mathrm{lossTNT}} = M_{\mathrm{lossRDX}}\frac{\rho_{\mathrm{TNT}}}{\rho_{\mathrm{RDX}}} \quad (5)$$

Figure 3 compares the measured and predicted cumulative dissolution rates for Particle 1. The agreement is quite good. Note that to obtain this good agreement we increased the effective surface area by a factor of 2 compared with a smooth cylinder to increase its dissolution rate (i.e., AF = 2 in eq 1). For the other three particles, AF = 1 produced good agreement with measured results.

Figure 3 also confirms the finding that the dissolution of RDX controls the dissolution of TNT in the Comp B particles. Independent dissolution of TNT would proceed much more quickly because both the solubility limit and the diffusion coefficient are about 3 times higher than those of RDX (eq 1).

To compare the measured and predicted dissolution rates for all Comp B particles, it is helpful to nondimensionalize eq 4

$$\frac{M_{\mathrm{loss}j}}{M_{0j}} = 2\left(\frac{t}{t_{0j}}\right) - \left(\frac{t}{t_{0j}}\right)^2 \quad (6)$$

where M_{0j} is the initial mass of species j in the particle and

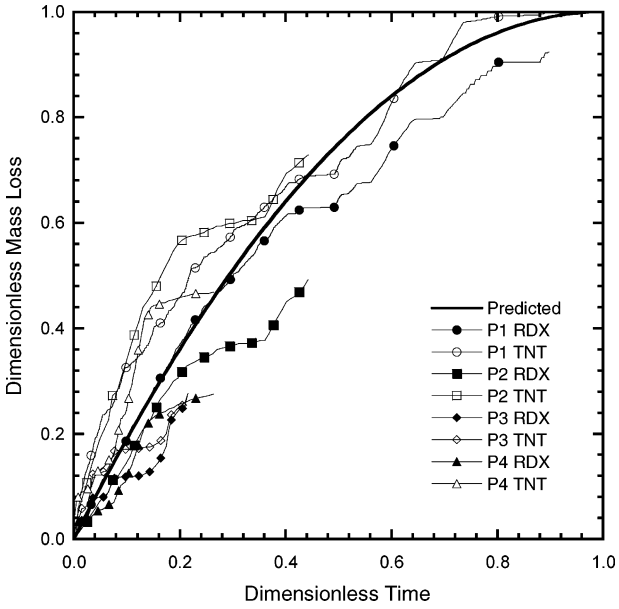

FIGURE 6. Dimensionless mass loss for each test particle vs dimensionless time compared with prediction based on a steady-flow model (eqs 6 and 7). The dissolution time used to scale test time is that for the RDX content in each particle.

t_{0j} is the dissolution time of species j in the particle (via eq 3)

$$t_{0j} = \frac{R_0^{3/2}}{B_j} \quad (7)$$

Figure 6 compares the predicted dimensionless mass loss versus time for the four test particles. Note that we used t_{0j} (or equivalently B_j) calculated for RDX to scale the test times for both RDX and TNT mass loss. The agreement is quite good for all four test particles, although only Tests 1 and 2 ran long enough to dissolve more than half of the initial particle masses.

Strictly speaking, the four test particles fall outside the range of validity of eq 1. For RDX at the average flow velocity (0.51 cm/h), eq 1 is valid for particles with radii larger than about 0.6 mm. The four particles had starting radii ranging from 0.43 to 0.18 mm, and the radii decreased as they dissolved during the tests. Nevertheless, agreement of the theory with the data is good, especially considering the general lack of tuning parameters.

Fast Percolation: Drop-Impingement Dissolution Model. When the percolation rate of water into the soil is fast, water will not pool on the surface during a rainstorm but disappear quickly into the ground. Raindrops impinging nearby will repeatedly wet an exposed HE particle. Between raindrops, the particle will hold a stagnant water layer against its surface, but otherwise the particle will not feel a mean flow. If this water layer is thin, then it will saturate, via diffusion, with dissolved HE before arrival of the next raindrop. The next drop will then wash away the dissolved HE and refresh the stagnant layer.

It is straightforward to model this process for a spherical particle. The time-dependent diffusion equation governs the HE saturation of a stagnant water layer on the particle

$$\frac{\partial c_j}{\partial t} = D_j\left(\frac{\partial^2 c_j}{\partial r^2} + \frac{2}{r}\frac{\partial c_j}{\partial r}\right) \quad (8)$$

The boundary conditions are $c_j = S_j$ on the particle surface $r = a$ and $\partial c_j/\partial r = 0$ on the outer surface of the water film

$r = b$. The initial condition is $c_j = 0$ for a new water layer. The water layer thickness is $h = b - a$.

Solutions to this problem (e.g., refs *22* and *23*) show that the water layer will saturate (average concentration > $0.9S_j$) for dimensionless time $D_j t/h^2 > 1$. The experiments had an average drip rate of about 20 drops per hour. For the case where RDX controls the dissolution of TNT, a water layer thinner than about 0.2 mm will saturate with RDX between drops. This is about the right scale for water layers observed on the test particles. The resulting mass of RDX and TNT in the saturated film is

$$\Delta M_{\mathrm{RDX}} = S_{\mathrm{RDX}} \frac{4}{3}\pi(b^3 - a^3) \tag{9}$$

$$\Delta M_{\mathrm{TNT}} = \Delta M_{\mathrm{RDX}} \frac{\rho_{\mathrm{TNT}}}{\rho_{\mathrm{RDX}}} \tag{10}$$

Equation 10 maintains the mean RDX/TNT ratio of the Comp B particle throughout dissolution and enforces the assumption that dissolution of RDX controls the dissolution of the particle.

The mass loss per drop is discrete rather than continuous. However, the incremental changes are small, and we may approximate this as a continuous process using the average mass-loss rate over time interval t_{d} between drops

$$-\frac{\mathrm{d}M_j}{\mathrm{d}t} \approx \frac{\Delta M_j}{t_{\mathrm{d}}}$$

$$-\rho_j 4\pi a^2 \frac{\mathrm{d}a}{\mathrm{d}t} = \frac{1}{t_{\mathrm{d}}} S_j \frac{4}{3}\pi[(a+h)^3 - a^3] \tag{11}$$

Equation 11 may be integrated, assuming h is a constant, to obtain the time to dissolve to a particle to a given size. In dimensionless form, the solution is

$$\begin{aligned} T(x_0,x) &\equiv \frac{S_j}{\rho_j}\frac{t}{t_{\mathrm{d}}} \\ &= \left[x_0 + \frac{1}{\sqrt{3}}\arctan(\sqrt{3}(1+2x_0)) - \right. \\ &\qquad \left. \frac{1}{2}\ln(1 + 3x_0 + 3{x_0}^2)\right] - \\ &\left[x + \frac{1}{\sqrt{3}}\arctan(\sqrt{3}(1+2x)) - \frac{1}{2}\ln(1+3x+3x^2)\right] \end{aligned} \tag{12}$$

where $x \equiv a/h$ and the subscript zero denotes initial conditions. Equation 12 cannot be inverted to solve for particle size as a function of time. Thus, to collapse the test data, it is convenient to plot dimensionless mass loss versus dimensionless time

$$\overline{M}_{\mathrm{loss}j} = 1 - \frac{M_j(a)}{M_{j0}} = 1 - \left(\frac{a}{a_0}\right)^3 \tag{13}$$

$$\frac{t}{t_0} = \frac{T(x_0,x)}{T(x_0,0)} \tag{14}$$

where the dissolution time is

$$\begin{aligned} t_0 = t_{\mathrm{d}}\frac{\rho_j}{S_j}\Big[x_0 + \frac{1}{\sqrt{3}}\arctan(\sqrt{3}(1+2x_0)) - \frac{1}{2}\ln(1+3x_0 + \\ 3{x_0}^2) - \frac{1}{\sqrt{3}}\arctan\sqrt{3}\Big] \end{aligned} \tag{15}$$

We do not know the exact thickness of the water layer and whether it varies with particle size. At present, this parameter must to be determined by fitting the test data, and selecting $h = 0.2$ mm for Particle 1 and $h = 0.1$ mm for the other three particles produces good agreement (Figure 7). With these parameters, the drop-impingement model collapses the data as well as the slow-percolation model.

Note that this model also predicts that independent diffusion of TNT and RDX into the stagnant water layer would cause faster than observed dissolution of the TNT in Comp B. The saturated mass of TNT in the layer would increase to

$$\Delta M'_{\mathrm{TNT}} = S_{\mathrm{TNT}} \frac{4}{3}\pi(b^3 - a^3) = \frac{S_{\mathrm{TNT}}}{S_{\mathrm{RDX}}}\frac{\rho_{\mathrm{RDX}}}{\rho_{\mathrm{TNT}}}\Delta M_{\mathrm{TNT}} \tag{16}$$

For the four test particles, this model indicates that the rate for independent dissolution of TNT would be 2−5 times higher than that when the dissolution of RDX controls the TNT rate. As with the steady-flow model, the resulting predictions would not fit the observed data.

The models presented here offer analytical predictions for the dissolution time of Comp B under the action of rainfall as functions of particle size or mass (eqs 7 and 15). Figure 8 shows the resulting predictions for nominal Comp B composition (RDX/TNT = 1.54) and the following model inputs: cylindrical particles, $R/L = 0.3$, $U = 0.55$ cm/h, AF = 1.5 for the slow-percolation model, and spherical particles, $h = 0.15$ mm, 20 drops/h for the drop-impingement model. The good fit of the models to the test data allows cautious extrapolation beyond the range of the test particles. The predicted dissolution times for the four test particles differ from the curves because they use particle-specific parameters for the RDX/TNT ratio, cylinder aspect ratio, AF, and h. Also, the predictions in Figure 8 do not include any time delay for the dissolution of waxy outer layers. Such factors could be included using statistics from the dissolution of a larger number of test particles.

Comparisons with Other Dissolution Studies. Matysliela (*21*) modeled the dissolution of a cylindrical block of Comp B in contact with porous soil. The model included both diffusion and advection of RDX and TNT through a boundary layer adjacent to the Comp B block. The advection model derives from Chambre et al. (*19*, *20*) and is identical to the steady-flow model presented here except Makysiela assumed that RDX and TNT dissolve independently. Consequently, the predicted TNT dissolution rate is much faster than that of RDX, contrary to our findings. As expected, Matyskiela found that mass loss by diffusion is much slower than that by advection for all cases modeled. Matyskiela also pointed out that mass-loss based on annual average flow, rather than "burst" rainstorm flow, overpredicts loss rates. This is because dissolution rate increases as $U^{1/2}$ (eq 1) while duration decreases as U for the same total annual rainfall.

Phelan et al. (*12*) layered Comp B particles within a matrix of glass beads in a cylindrical column and subjected them to steady water flow (0.16−0.70 cm/h). The particles were manufactured from bulk Comp B and sieved to produce narrow size distributions centered on 0.1 and 1 mm. Micrographs showed fine HE dust adhering to the surfaces of the particles. The concentration of TNT and RDX in the effluent was measured at regular intervals, and residuals in the glass-bead matrix were measured at the end of each test. We would expect these results to follow predictions based on the steady-flow model presented here. Unfortunately, direct comparison has proven difficult. Bed loading was sufficiently high in many cases that interaction between Comp B particles probably occurred. Also, the HE surface dust would have dissolved rapidly at the onset of each test, accounting for initial concentration spikes. Recovered RDX ranged from 59% to 174% of initial RDX mass, and recovered TNT ranged from 35% to 89% of initial TNT mass. The authors

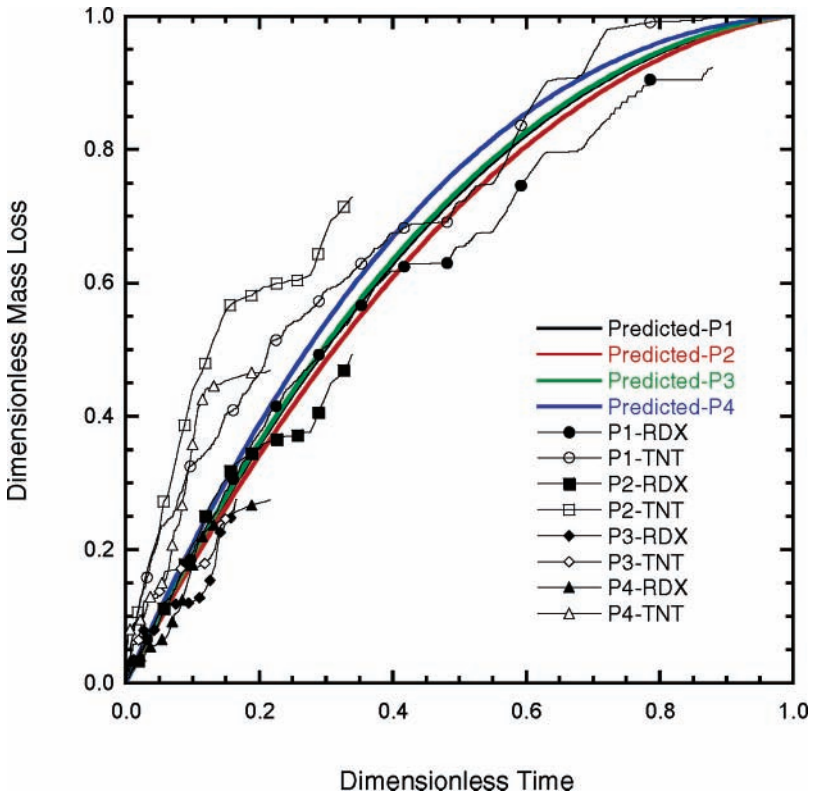

FIGURE 7. Dimensionless mass loss for each test particle vs dimensionless time compared with prediction based on the drop-impingement model (eqs 12−15). The small differences between the predicted curves reflect different values of the ratio of initial particle size to layer thickness, $x_0 = a_0/h$.

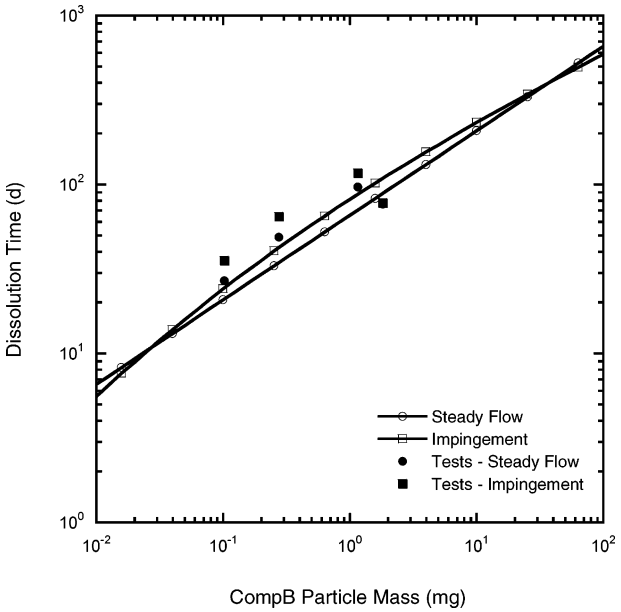

FIGURE 8. Predicted dissolution time (rainfall days) vs particle size for steady-flow and drop-impingement models based on nominal Comp B composition, rainfall of 0.55 cm/h or 20 drops/h, and AF = 1.5 (steady) and $h = 0.15$ mm (drip). Also shown are the predicted dissolution times for the four test particles, using particle-specific parameters.

could not account for these discrepancies, which make it difficult to quantify dissolution times and mass-loss profiles.

Despite these shortcomings, some comparisons are possible. Two representative tests that used low bed loading (MT8c and MT16) indicate that TNT dissolved about twice a fast as RDX, not 6.7 times faster as predicted by eq 1 for independent dissolution. Also, the dissolution rates during both tests did not decrease linearly with time, as predicted by eqs 1 and 3, but flattened out as the tests progressed. Because the test particles consisted of size ranges, the smaller particles would dissolve quickly, and the dissolution rate would flatten out as only larger particles remain.

Lynch et al. (*11*) cast TNT and Comp B into disks (5.5 cm in diameter × 0.88 cm thickness) and measured their initial dissolution rates in a fixed water volume stirred at a constant rate. They also measured the dissolution rates of pure RDX and TNT particles dissolved separately and in unbound mixtures in the same proportions as found in Comp B. They normalized the measured rates by the measured or calculated area of the constituents exposed on the surface of the samples. While interesting, these experiments are difficult to compare with those conducted here. The experiments obtained the initial dissolution rates of TNT and RDX in Comp B and did not track changes as the particles dissolved and varied in size, surface texture, and composition. Also, the method described by Lynch et al. (*10*) to equate mixing power with rainfall power uses empirical correlations not easily applied to our tests. An important result, that dissolution rate per unit area for TNT in Comp B is significantly lower than that for pure TNT flakes, seems reasonable. However, they also found that the cast TNT samples had lower dissolution rates per unit area than those of pure TNT flakes. Similarly, the RDX in Comp B had lower dissolution rates per unit exposed surface area than those of pure RDX. Lynch et al. do not explain why the surface area corrections do not collapse these results.

Discussion

We designed our experiments to mimic rainfall-driven dissolution of HE residuals deposited on surface soils of firing ranges. They are the first experiments to dissolve individual HE particles collected from the detonation of live munitions, to drip water onto the particles, and to track changes in the

particles as dissolution proceeds. These features have proven to be important.

The Comp B detonation residuals were from blow-in-place, low-order detonations that should replicate live-fire, low-order detonations. The particles had a variety of surface textures and RDX/TNT ratios. The onset of dissolution was delayed for two of the four test particles, apparently owing to surface texture. Initially, we thought that the different particle RDX/TNT ratios were due to their heating histories. However, separate chemical analyses of crystalline grains and melt spheres are not significantly different (*4*). Comp B particles from the same detonation do, however, have similar RDX/TNT ratios. The 30 analyzed particles (Table 1) and Particle 1 came from detonation LO-a. These have RDX/TNT ratios of 1.74 ± 0.28 while Particles 2, 3, and 4 from detonation LO-b have RDX/TNT ratios 1.19 ± 0.23. We suggest that either the original composition of a round or the specifics about how it detonated affected the RDX/TNT ratios in the residuals. These effects would not be seen for test particles manufactured from bulk Comp B.

Detonations scatter HE residuals onto the surface of firing ranges at very low spatial concentrations. Energy differences suggest that the particles are not likely to be covered by soil from the same detonation. They are subsequently exposed directly to rainfall, and each particle dissolves independently. The arriving rain drops can impinge directly on a particle or they can inundate a particle and produce a slow, steady flow. Our apparatus focuses on dissolution of surface-deposited particles and can mimic either flow regime.

At the onset of the dissolution of Comp B, surface TNT quickly dissolves, leaving exposed RDX crystals that impede further dissolution of TNT. Particle texture quickly changes from relatively smooth to lumpy. Subsequently, the dissolution rates of the two components and their ratio in the effluent can both vary by an order of magnitude on short time scales (hours). This reflects the relative exposed areas of the two compounds and intermittent release of an RDX crystal. On longer time scales (days), the relatively slow dissolution of RDX controls dissolution of TNT and the Comp B particle as a whole by limiting the exposed surface area of TNT. These characteristics have not been reported previously and have not been considered when determining dissolution times for Comp B residuals. Importantly, they are not replicated by measuring the initial dissolution rates of Comp B particles of different average size. Also, these characteristics are difficult to discern when numerous Comp B particles are dissolved at once.

The finding that the relatively slow dissolution of RDX controls dissolution of Comp B seems intuitively reasonable. It suggests that TNT diffuses very slowly through RDX and can only dissolve at locations where it is directly exposed to water. Local dissolution of TNT exposes more RDX and less TNT surface area, slowing down the dissolution of TNT. The exposed areas of RDX and TNT in a particle can vary broadly during the experiment, including times when an RDX crystal falls off the Comp B particle. These effects cause the wide variation of RDX/TNT in the effluent. However, overall the TNT dissolves at a rate that approximately maintains the average RDX/TNT ratio of the particle, with the time scale controlled by dissolution of exposed RDX. Exceptions include the initial rapid dissolution of exposed TNT and final stages when nearly all of the TNT remaining is exposed or only RDX remains. A similar finding should apply for other HE mixtures with components that dissolve at different rates, for example, Octol (70% HMX, 30% TNT).

The two dissolution models presented here attempt to bracket the behavior of an HE particle on porous soil exposed to rainfall. The suitability of one or the other will depend on soil permeability relative to rainfall rates at the sites of interest. For slow percolation of rain into the soil, the particle will experience relatively steady flow at a low Reynolds number. The steady-flow model based on that developed by Chambre et al. (*19*, *20*) should work well for this case. For rapid percolation of rain into soil, individual raindrops falling near the particle will cause dissolution, and the drop-impingement model developed here should work well. For simple particle geometries, the models yield analytical expressions for dissolution rates and times. Control of particle dissolution by the slowest dissolving component is easy to implement by using that component's parameters for time-scale calculations.

Both models agree well with our test data, and dimensionless predictions collapse the dissolution time sequencees for all four particles. They each predict that independent dissolution of TNT would cause TNT loss rates to be several times faster than observed rates. The models can be applied to predict dissolution of single-component HE residues, such as TNT, and other compositions consisting of slow- and fast-dissolving components. They can also be applied using site-specific soil permeability and rainfall data. The steady-flow model can also be applied to the case of HE particles buried in porous soil by simply selecting an appropriate porosity (the intended use of the original model by Chambre et al. (*19*, *20*)).

The models rely primarily on well-known parameters for the constituent compounds, such as solubility, diffusivity, and density. A single tuning parameter, area factor (AF) for the steady-flow model and layer thickness (h) for the drop-impingement model, must derive from direct measurements or fitting to dissolution data. Variations in these parameters should reflect physiochemical differences in the particles. However, detonations release thousands of particulate residuals. While desirable, linking AF and h to physiochemical features then would require linking those features to detonation processes to predict their statistics. At present, we think obtaining AF and h statistics by fitting the models to dissolution data is more practical.

These models offer promising methods to predict dissolution rates for HE particles on firing ranges. However, they have been validated using only four test particles. More tests are needed to assess the variability in the tuning parameters, to confirm the predicted time sequences, and to improve confidence in predicted dissolution times outside the range of particle sizes tested here. As mentioned, dissolution rates in the two models have different dependence on rainfall. The dissolution rate varies with average rainfall rate ($U^{1/2}$) for the steady-flow model and drop arrival rate ($1/t_d$) for the drop-impingement model. However, these are not independent parameters but are linked by rainfall physics; drop sizes and arrival rates increase with increasing rainfall rates (*16*). Thus, a sensitivity study to assess the differences between the two models should include this interdependence of rainfall parameters. Also, the models describe only dissolution of HE particles and do not address other factors such as sorption, dispersion, and dilution that influence the transport of the explosives. These effects must be addressed to obtain reliable predictions for HE concentrations in groundwater at training ranges.

Acknowledgments

We thank Chuck Daghlian for the use of the scanning electron microscope at Dartmouth College, Nicole West for running some of our HPLC analyses, and the Army Environmental Center for funding this work.

Literature Cited

(1) Environmental Protection Agency. *In the Matter of Training Range and Impact Area, Massachusetts Military Reservation. Administration Order for Response Action*; EPA Docket Number SDWA-1-2000-0014; U. S. EPA Region 1: 2000.

(2) Jenkins, T. J.; Pennington, J. C.; Ranney, T. A.; Berry, T. E., Jr.; Miyares, P. H.; Walsh, M. E.; Hewitt, A. D. *Characterization of Explosives Contamination at Military Firing Ranges*; ERDC Technical Report TR-01-5; Cold Regions Research and Engineering Laboratory, Hanover NH, 2001.
(3) Taylor, S.; Hewitt, A.; Lever, J.; Hayes, C.; Perovich, L.; Thorne, P.; Daghlian, C. TNT particle size distributions from detonated 155-mm howitzer rounds. *Chemosphere* **2004**, *55*, 357−367.
(4) Taylor, S.; Lever, J. H.; Perovich, L.; Campbell, E.; Pennington, J. A study of Composition B particles from 81-mm mortar detonations. In *Proceedings of the Conference on Sustainable Range Management*, New Orleans, LA, 2004.
(5) Hewitt, A. D.; Jenkins, T. F.; Ranney, T.; Stark, J.; Walsh, M. E.; Taylor, S.; Walsh, M.; Lambert, D.; Perron, N.; Collins, N.; Karn, R. *Estimates for Explosive Residue Deposition from the Detonation of Army Munitions*; ERDC/CRREL TR-03-16; 2003.
(6) Radtke, C. W.; Gianotto, D.; Roberto, F. F. Effects of particulate explosives on estimating contamination at a historical explosives testing area. *Chemosphere* **2002**, *46*, 3−9.
(7) Brannon, J. M.; Pennington, J. C. Environmental Fate and Transport Process Descriptors for Explosives; ERDC/EL TR-02-10; U. S. Army Engineering Research and Development Center: Vicksburg, MS, 2002.
(8) Ro, K. S.; Venugopal, A.; Adrian, D. D.; Constant, D.; Qaisi, K.; Valsaraj, K. T.; Thibodeaux, L. J.; Roy, D. Solubility of 2,4,6,-trinitrotoluene (TNT) in water. *J. Chem. Eng. Data* **1996**, *41*, 758−761.
(9) Lynch, J. C.; Myers, K. F.; Brannon, J. M.; Delfino, J. J. Effects of pH and temperature on the aqueous solubility and dissolution rate of TNT, RDX and HMX. *J. Chem. Eng. Data* **2001**, *46*, 1549−1555.
(10) Lynch, J. C.; Brannon, J. M.; Delfino, J. J. Dissolution rates of three high explosive compounds: TNT, RDX and HMX. *Chemosphere* **2002**, *47*, 725−734.
(11) Lynch, J. C.; Brannon, J. M.; Delfino, J. J. Effect of component interactions on the aqueous solubilities and dissolution rates of the explosive formulations Octol, Composition B and LX-14. *J. Chem. Eng. Data* **2002**, *47*, 542−549.
(12) Phelan, J. M.; Webb, S. W.; Romero, J. V.; Barnett, J. L.; Griffin, F.; Eliassi, M. *Measurement and Modeling of Energetic Material Mass Transfer to Soil Pore Water—Project CP-1227*; Sandia Report 2003-0153; 2003.
(13) Pennington, J. C.; Jenkins, T. F.; Ampleman, G.; Thiboutot, S.; Brannon, J. M.; Lewis, J.; Delaney, J. E.; Clausen, J.; Hewitt, A. D.; Hollander, M. A.; Hayes, C. A.; Stark, J. A.; Marois, A.; Brochu, S.; Dinh, H. Q.; Lambert, D.; Martel, R.; Brousseau, P.; Perron, N. M.; Lefebvre, R.; Davis, W.; Ranney, T. A.; Gauthier, C.; Taylor, S.; Ballard, J. M. *Distribution and Fate of Energetics on DoD Test and Training Ranges: Report 3*; ERDC/EL TR-02-EL-191; 2003.
(14) Environmental Protection Agency. *Nitroaromatics and Nitramines by HPLC*, second update; SW-846 Method 8330; 1994.
(15) U. S. Army Material Command. *Engineering Design Handbook, Explosives Series, Properties of Explosives of Military Interest*; Pamphlet AMCP 706-177; Army Material Command Headquarters: Washington, DC, 1971.
(16) Pruppacher, H. R.; Klett, J. D. *Microphysics of Clouds and Precipitation*; Kluwer Academic Publishers: Boston, 1997.
(17) Buttle, J. M. Isotope hydrograph separations and rapid delivery of pre-event water from drainage basins. *Prog. Phys. Geogr.* **1994**, *18*, 16−41.
(18) Taylor S.; Feng, X.; Williams, M.; McNamera, J. Estimating the isotopic composition of snowmelt for hydrograph separation. *Hydrol. Processes* **2002**, *16*, 3683−3690.
(19) Chambre, P. L.; Pigford, T. H.; Futjita, A.; Kanki, T.; Kobayashi, A.; Lung, H.; Ting, D.; Sato, Y.; Zavoshy, S. J. *Analytical Performance Models for Geological Repositories*; LBL-14842; Lawrence Berkeley Laboratory, University of California: Berkeley, CA, 1982.
(20) Chambre, P. L.; Pigford, T. H. 1984 Prediction of waste performance in a geological repository. *Mater. Res. Soc. Symp. Proc.* **1984**, *26*, 985−1008.
(21) Matyskiela, W. *Modeling of Chemical Transport from UXO to Surrounding Soil*; final report submitted to Praxis Environmental Technologies; 2003.
(22) Skelland, A. H. P. *Diffusional Mass Transfer*; John Wiley and Sons: New York, 1974.
(23) Ozisik, M. N. *Heat Conduction*; John Wiley and Sons: New York, 1980.

Received for review March 16, 2005. Revised manuscript received July 10, 2005. Accepted August 29, 2005.

ES050511R